Damage Analysis of Utatsu Bridge Affected by Tsunami due to Great Eastern Japan Earthquake

Li FU[1], Kenji KOSA[2], Hideki SHIMIZU[3], Tatsuo SASAKI[4]

[1] Research Student, Dept. of Civil Engineering, Kyushu Institute of Technology
(804-8550, Sensui 1-1,Tobata, Kitakyushu, Japan)
[2] Ph.D., Professor, Dept. of Civil Engineering, Kyushu Institute of Technology
(804-8550, Sensui 1-1,Tobata, Kitakyushu, Japan)
[3] Senior Engineer, Structural Engineering Division, Nippon Engineering Consultants Co., Ltd
(Currently in the doctoral program at Kyushu Institute of Technology)
[4]Senior Engineer, Structural Engineering Division, Nippon Engineering Consultants Co., Ltd.

1. INTRODUCTION

The 2011 Tohoku Earthquake, known as the Great Eastern Earthquake as well, occurred at 2:46 p.m (JST) on March 11th with a magnitude 9.0. It was one of the most powerful earthquakes to have hit Japan. Besides that, the earthquake caused an extremely destructive tsunami wave which induced an extensive loss in Tohoku region. Many bridges in Tohoku region have suffered tremendous damage by tsunami. The authors have conducted a reconnaissance visit to the coast of Tohoku region to observe the damage condition of a number of bridges.

The Utatsu Bridge, located in the coast of Irimae Bay, is a 304m long, 8.3m wide, 12 spans, prestressed concrete bridge which consisted of 3 types of superstructures and the location of it is shown in **Fig.1**. Based on the detailed field survey it was observed that for the damage of superstructures the central 8 spans have been washed away by tsunami.

The detailed damage performance of Utatsu Bridge is presented in the following chapter and this paper also provides a method about how to obtain the wave flow velocity and wave height at Utatsu Bridge. Besides that, comparisons of wave acting effect and bridge resistance have been conducted to check the outflow of superstructures and to approach the damage condition of piers.

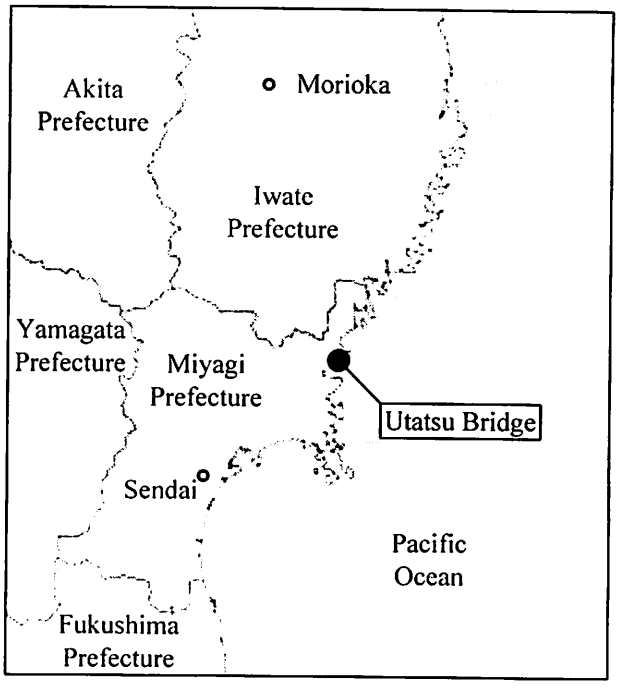

Fig.1 Location of Utatsu Bridge

2. DAMAGE SITUATION

(1) Introduction of Bridge Structure

The Utatsu Bridge, located at Minamisanriku Town over Irimae Bay, is composed of 3 types of superstructures varying in length from 14.4m to 40.7m, as shown in **Fig.2**. For simplicity, the authors assigned numbers for the superstructures and piers from Sendai side to Aomori side. The 12 superstructures were numbered from S1 to S12 while the 11 piers were numbered from P1 to P11.

2) Outflow Condition of Superstructures

Based on the detailed survey, superstructures S3~S10 moved off from their supports under the wave-induced lateral load while the superstructures of span1, span 2, span 11 and span 12 did not flow out. The displacements of S3~S10 have been illustrated in **Fig.3**. The directions of displacements are transverse to the bridge axis. The characteristic of outflow condition is that the central spans such S5~S7 and S8 experienced long displacements (28m and 41m). On the contrary, the side spans such as S1, S2, S11 and S12 did not flow out.

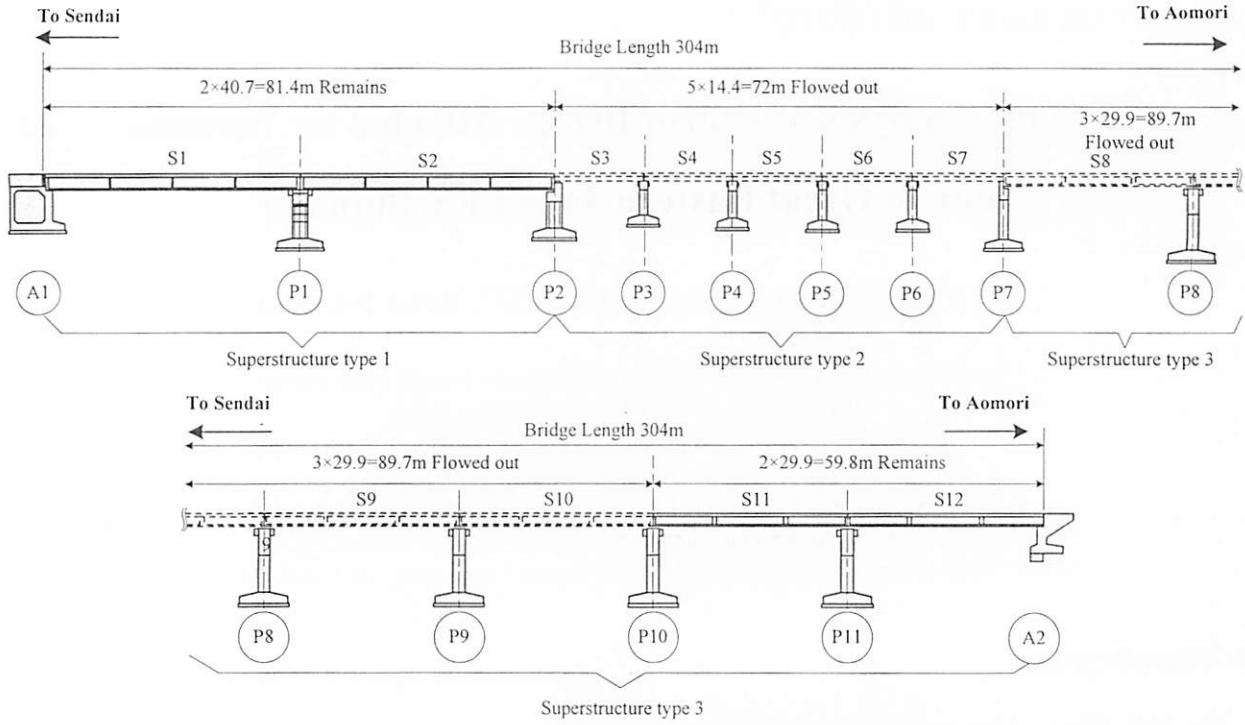

Fig2 Side View of Utatsu Bridge

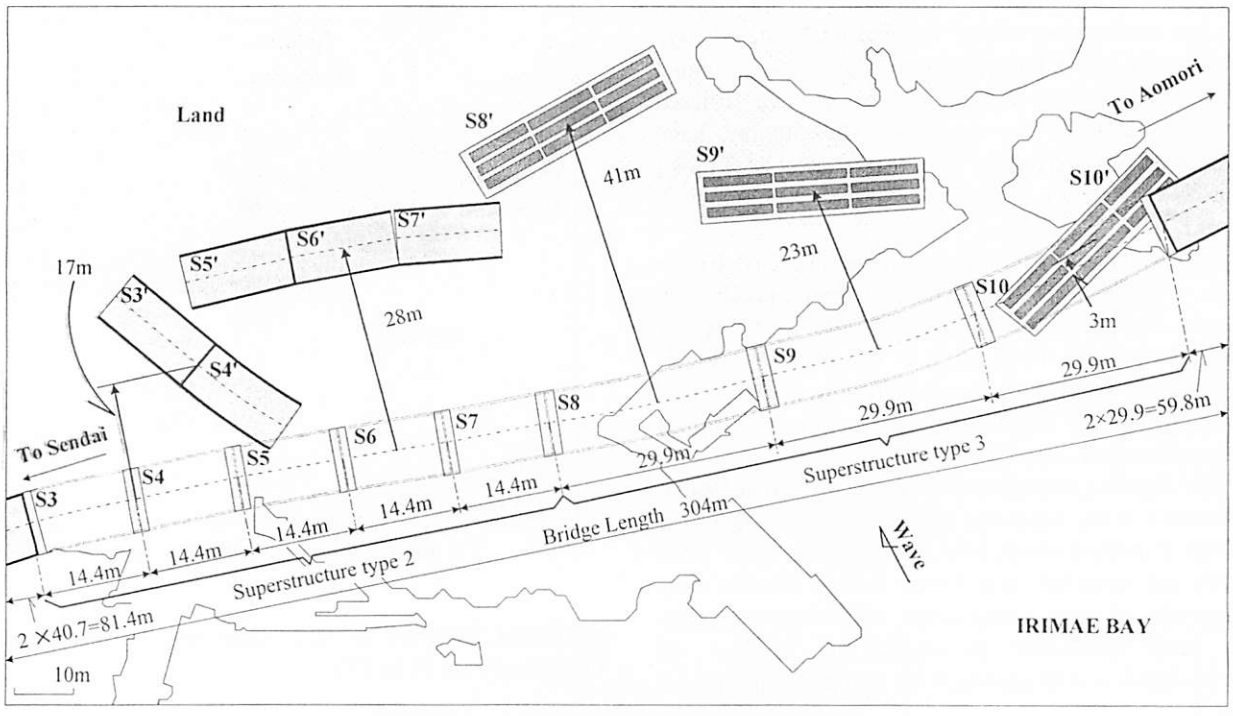

Fig.3 Outflow Condition of Utatsu Bridge

It was also observed that S3~S4 and S5~S7 flowed out with no separation. Due to a great wave-induced uplift force, S8~S10 were inverted when they moved off.

However, contrary to the damage of superstructures, during the tsunami attack, all piers of Utatsu Bridge withstand the wave action and did not collapse. The main damage of the piers is that the concrete surfaces of beams dropped due to a collision with girders and most of bridge collapse preventions were crushed or flowed out, refer to **Fig.4**.

(3) Detailed damage of Superstructures4

The damage of S3~S7 is one of the typical ones, which flowed out connecting with each other, and the damage of S6~S7 was selected as an example to state in the following content. Under the wave action, S6 and S7

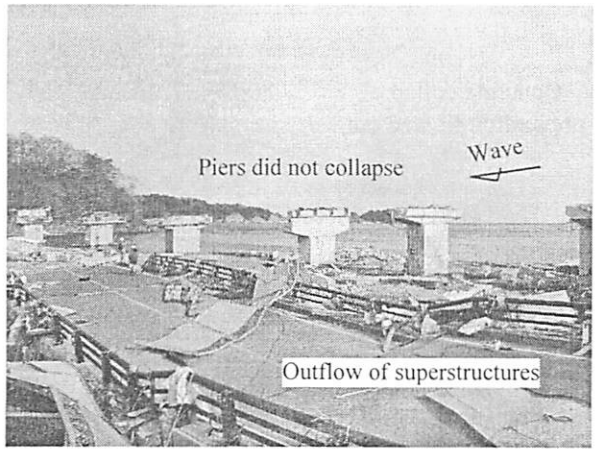

Fig.4 Damage of Piers

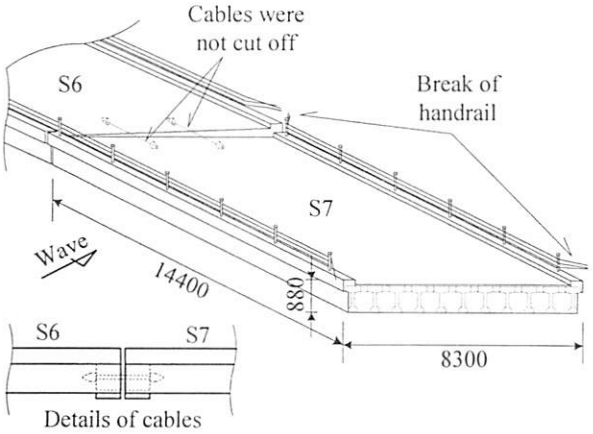

Fig.5 Detailed Damage of S6, S7

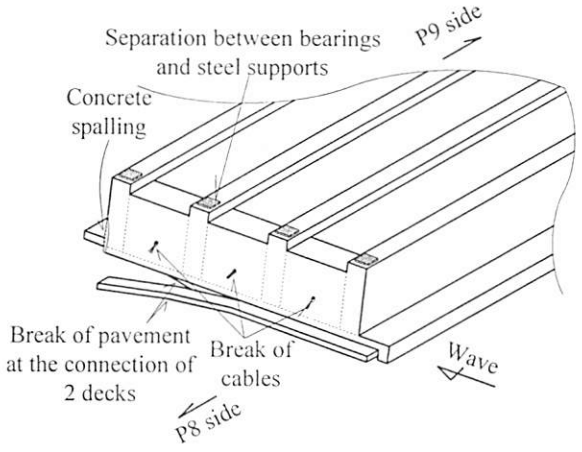

Fig.6 Detailed Damage of S9

experienced a displacement of 28m together thus it is proper to regard them as a whole. When the bridge was retrofitted, 2 cables, which were used to prevent the relative movement in axis direction of superstructures, were installed between S6 and S7. The details of the cables are plotted in **Fig.5**. These cables played an important role to keep S6 and S7 flowing out together. Besides that, the damage of handrail between S6 and S7

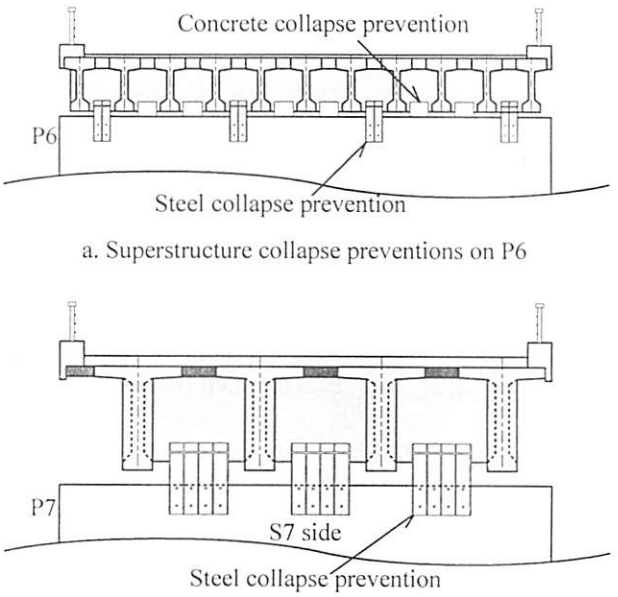

a. Superstructure collapse preventions on P6

b. Superstructure collapse preventions on P7

Fig.7 Details of Collapse Preventions on P6 and P7

was observed as well.

S9 is one of the inverted superstructures, the damage of which is shown in **Fig.6**. S9 experienced a displacement of 23m and was inverted by the wave-induced uplift. At the end surface of P8 side, different from the damage of S6 and S7, all of the cables which connected S8 and S9 were broken by the force between superstructures and the fracture traces could be found. Moreover, at the supporting area of girders, the remains of bearing plates were noted. In light of this, it is obvious that during the tsunami attack the bearings fractured. Besides that, at the connection of the 2 decks, the debris of pavement connection was observed.

(4) Detailed Damage of Piers

It was found that the 11 piers supported 3 types of superstructures. In this section, 3 piers were selected basing on their different supporting superstructures. Pier 6 and Pier 8 respectively supported the type 2 and type 3 and in contrast, Pier 7 supported both of these 2 types of superstructures, illustrated in **Fig.2**. Therefore P6~P8 were selected to analyze. For P6 and P7, except for the concrete collapse preventions, they also had been installed steel preventions the installing details of which are shown in **Fig.7**. Different from P6 and P7, only concrete collapse preventions were set up at the top of P8. These collapse preventions not only limit the superstructure's movement along the axis direction but also the transverse direction of bridge.

The detailed damage of P6 is shown in **Fig.8**. When S6 and S7 were separated from P6, they imposed a horizontal collision on the concrete collapse preventions. Therefore, on the supporting plate of P6, 12 concrete collapse preventions were crushed. And for the same reason, the 8 steel collapse preventions, anchored on the sides of the beam, flowed out as well. Apart from the

damage of the collapse preventions, the concrete surface of the beam which was located at the land side was also crushed.

Fig.9 illustrates the detailed damage of P7 which supported 2 types of superstructures: S7 and S8. At S7 side, the installing details of superstructure collapse preventions were same as P6. Although the 6 concrete collapse preventions were crushed, the 4 steel ones were left. However, due to the girder-induced impact, the steel ones tilted. At S8 side, different from P6, only 3 larger steel collapse preventions were anchored and they did not flow out. The damage condition of steel collapse preventions demonstrates that when the superstructures, located on P7, displaced they were elevated by a wave-induced uplift. Because of this, the superstructures flowed from the top of the steel collapse preventions and did not impose a sufficient impact to make them separate from supports. Besides that, at the land side, the concrete surface of the beam was crushed and some steel bars could be observed.

The damage of P8 is plotted in **Fig.10**. On the top of beam, 6 concrete collapse preventions and 2 side concrete blocks had been set up. For the same force situation as the preventions of P6, the 6 concrete collapse preventions and one side block, which was at the land side, were crushed. Besides that, it was found that while the side block flowed out, a damage of the concrete surface, which under the side block, occurred.

3. DETERMINATION OF WAVE FLOW VELOCITY AND HEIGHT

In order to evaluate the wave action on bridge superstructures and piers, it is necessary to obtain the wave flow velocity and height at Utatsu Bridge. Due to the lack of the wave velocity and height, a measurement was conducted by authors. 12 videos which recorded the tsunami attack in Minamisanriku City and Sendai City were collected and based on these video records, the shooting locations of which is shown in **Fig.11**, a measurement of wave flow velocity and height was conducted.

(1) Determination of Wave Flow Velocity

For instance, in a video the authors were able to search for 2 distinguished place points where a piece of floating debris passed through. By using Google Earth's distance measurer and the timer in the video, it is possible to obtain the distance and the time span for the floating debris flowed from one place point to the other. At last the kinematics Equation (1) was applied to calculate the velocity of the floating debris which is assumed to be the wave flow velocity.

$$v = \frac{S}{t} \qquad (1)$$

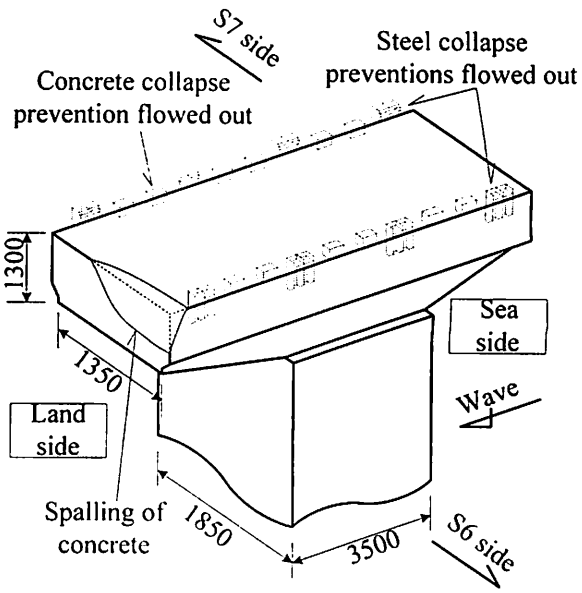

Fig.8 Detailed Damage of P6

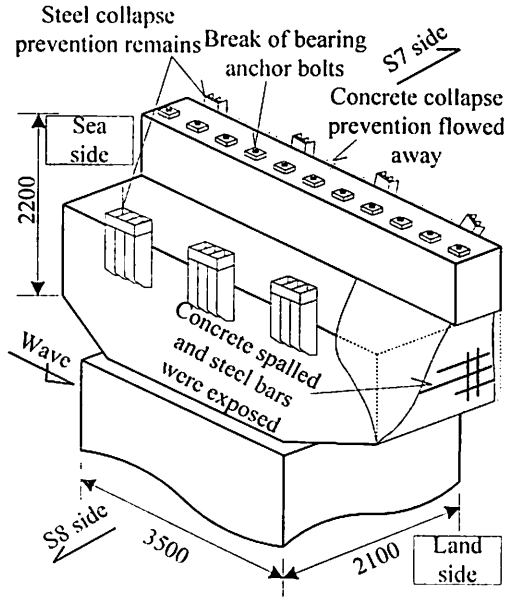

Fig.9 Detailed Damage of P7

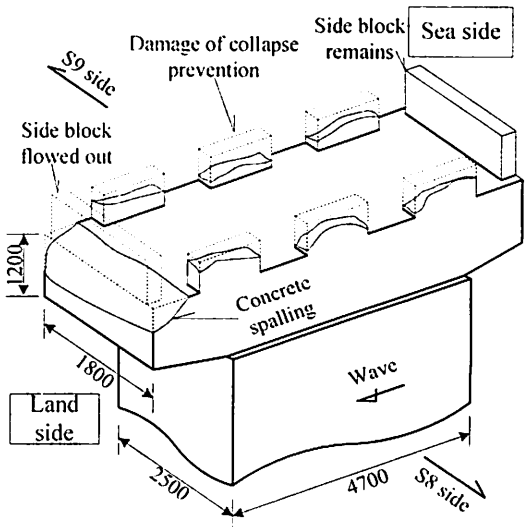

Fig.10 Detailed Damage of P8

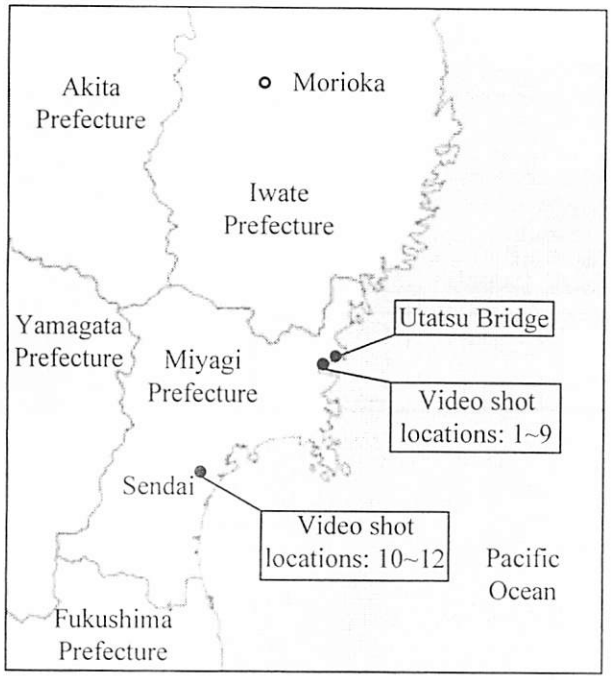

Fig.11 Video Shot Locations

Where,

v is wave flow velocity (m/s); S is the distance between 2 place points (m); t is the time span for the debris flowing from one point to the other.

In this paper, the velocity calculation of location 1, which is about 7.5km south west from Utatsu Bridge, is shown as an example. As shown in **Fig.12**, the flow of the floating debris was recorded. The distance from point 1 to point 2, which the debris passed through, was measured as 63m. When the debris passed point 1, the timing was starting and while it passed point 2 the timing was over. Based on the video's timekeeper, t=10s was obtained, as shown in **Fig.13**. In the end, by using the Equation (1), the wave flow velocity at location 1 was calculated as 6.3m/s. By the same method, 12 groups of velocity data are available, illustrated in **Fig.14**.

Owing to the lack of the video data at the Utatsu Bridge, the authors assumed the wave velocity at Utatsu Bridge by using the 12 groups of data in other places. From **Fig.14**, it is observed that the maximum, average, and minimum velocities are respectively 7.0m/s, 5.4 m/s, and 4.0m/s. Combining the huge losses of the Utatsu Bridge, it is proper to assume the velocity at Utatsu Bridge as 6.0m/s, which is slightly larger than the average velocity.

(2) Determination of Wave Height

The wave height was able to be determined as well by using video records. An evaluating example at S12 of the Utatsu Bridge was stated. Depending on the video record, the height from the wave top surface to the top of handrail (h) was able to be roughly determined as 0.4 m, refer to **Fig.15**.

After h was obtained, combining the detailed dimensions of the bridge and the sea level before wave coming, it is available to determine the wave height as

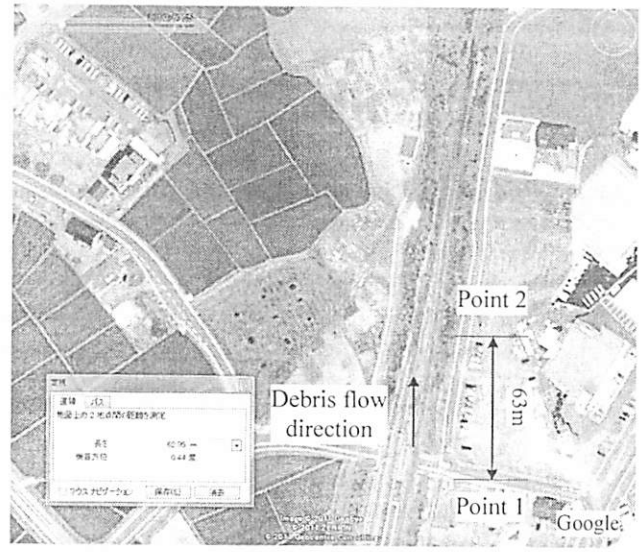

Fig.12 Displacement of the Debris Recorded at Location 1 (by Google Earth)

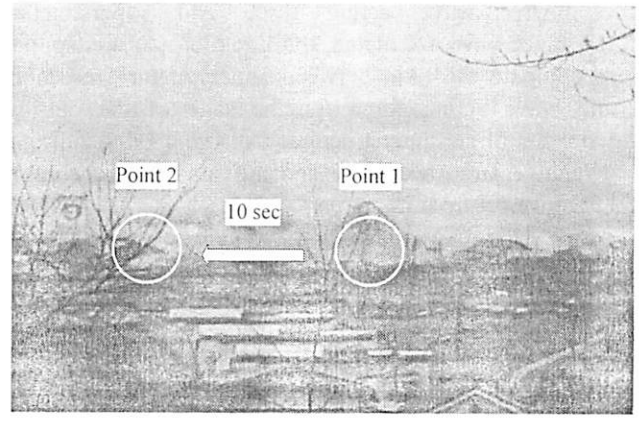

Fig.13 Time Span for the Debris Flowed from Point 1 to Point 2 (by the video on Youtube)

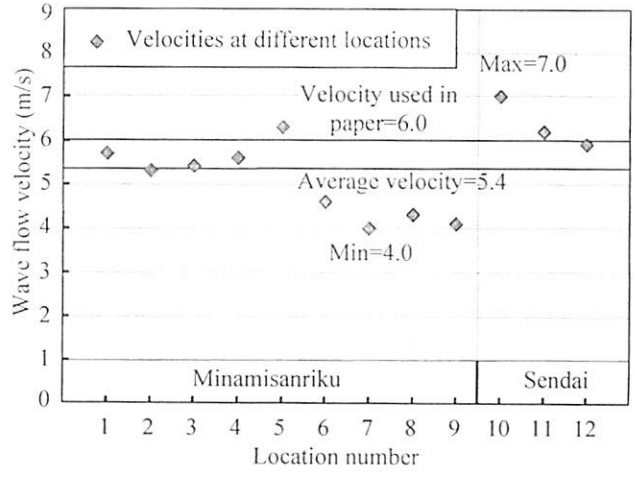

Fig.14 Calculating Result of Wave Velocity

8.4m. Utilizing the same method, the wave heights of all spans could be roughly determined.

4. JUDGMENT OF SUPERSTRUCTUREWS OUTFLOW

(1) Outflow Judgment by the Comparison of Wave Acting Force and Frictional Resistance

In this chapter, the simple judging equations were applied to evaluate the outflow of superstructures. In order to judge the outflow of superstructures, the concept of ratio β between superstructure resistance and wave acting force was utilized[1]. The wave acting force could be calculated by Equation (2), in which the wave flow velocity had been verified as 6.0m/s, as mentioned in Chapter 3, and the resistant coefficient C_d was determined according to the Japanese specification[2]. The superstructure resistance against wave force could be calculated by the product of the frictional coefficient and the superstructure weight, according to Equation (3).The frictional coefficient was assumed as 0.6, depending on the experimental result of the research[3]. Because when the wave was about to affect on the superstructures, no wave buoyancy acted on the bottoms of superstructures, the buoyancy was not considered in Equation (3).

After wave acting force and superstructure resistance were calculated, the Equation (4) was applied to compute the ratio between superstructure resistance and wave acting force for the sake of the outflow judgment of the superstructures. A large β value indicates a relative large resistance and the superstructure might not move off from its support.

$$F = \frac{1}{2} \cdot \rho_w C_d v^2 A \tag{2}$$

$$S = \mu W \tag{3}$$

$$\beta = \frac{S}{F} \tag{4}$$

3 different β values have been calculated, because the Utatsu Bridge consists of 3 types of superstructures, illustrated in **Fig.16**. Based on the survey report[4], the average β value of the bridges, located at the Tohoku area, which suffered serious dislocations, is 0.84. The β values of the Utatsu Bridge are 1.03, 0.90 and 0.83, which are close to 0.84. Therefore, it is sufficient for the wave acting force to make S3~S10 move off.

(2) The Relation between Superstructure Flowing Acceleration and Displacement

A further study was conducted to care, at different acceleration cases when superstructures were flowing out, the corresponding damage degrees of superstructures. Taking buoyancy effect into account, the authors have tried to find out the relation between superstructure accelerations and displacements. Equation (6) is derived from Equation (5) and at the right side of the Equation (5), the first item is wave acting force and the second item is superstructure resistance. Superstructure flowing accelerations could be calculated from Equation (6). Equation (7) expresses that the displacements of the superstructures are decided by their accelerations and the time spans they moved.

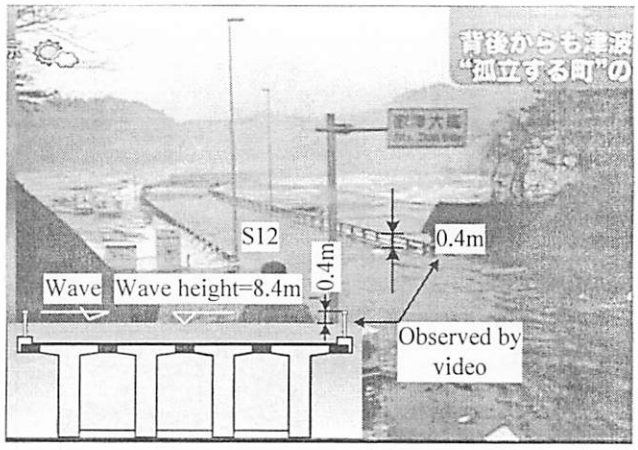

Fig.15 Calculation of the Wave Height at S1 (by the video on Youtube)

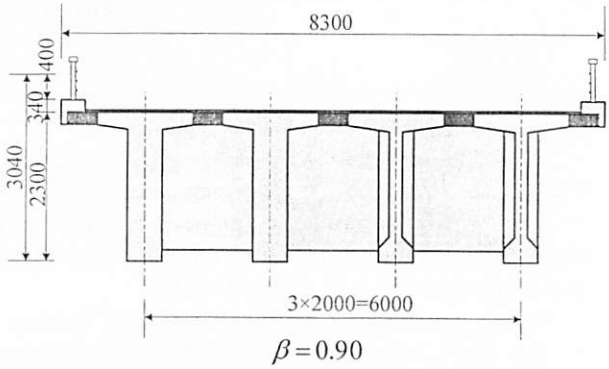

$\beta = 0.90$

(a) Superstructure type 1: S1~S2

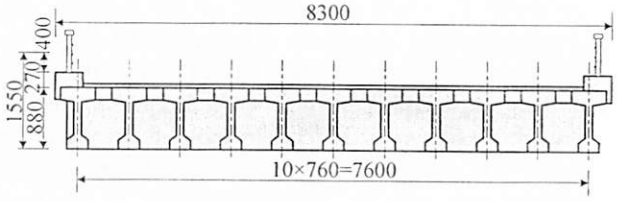

$\beta = 1.03$

(b) Superstructure type 2: S3~S7

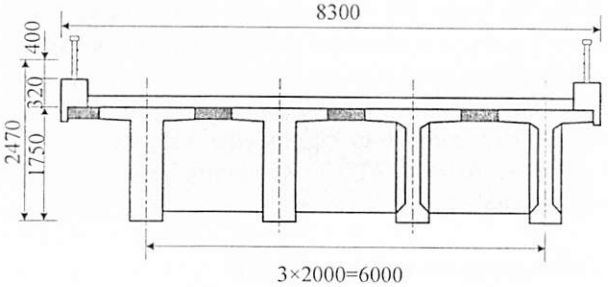

$\beta = 0.83$

(c) Superstructure type 3: S8~S12

Fig.16 β Values of 3 Types of Superstructures

$$m\alpha = \frac{1}{2}\rho_w C_d v^2 A - \mu(mg - \rho_w g l') \quad (5)$$

$$\alpha = [\frac{1}{2}\rho_w C_d v^2 A - \mu(mg - \rho_w g V)] / m \quad (6)$$

$$L = \frac{1}{2}\alpha t^2 \quad (7)$$

Where,

α is superstructure flowing acceleration induced by horizontal wave effect (m/s^2); m is the quality of superstructure (kg); g is gravity acceleration (m/s^2); V is the volume of superstructure (m^3); L is the displacement of superstructure (m).

The calculating result is plotted in **Fig.17**. It is found that the superstructures S1, S2, S11and S12 did not experience movements although their calculating accelerations are larger than S3~S7 and the possible reason is that for these spans, some huge obstacles in front of superstructures reduced the wave flow velocity which caused a decrease of acting force on these spans. By ignoring the superstructures which did not displace, it is found that the displacements of superstructures which had a same acceleration are relatively different. For example, S8 moved 41m while S10 moved 3m although they had the same acceleration. The possible reason was put forward. Based on **Fig.2**, it is obvious that from the middle span to side spans the displacements reduce gradually from 41m to 0m, which expresses the wave acting force kept the same trend. Therefore, in reality, the acceleration of S8 should have been larger than S10 which resulted in their distinguished displacements.

5. JUDGMENT OF PIER DAMAGE

(1) Damage Judgment of Pier 8

All of the piers of Utatsu Bridge did not collapse under the effect of tsunami. During the Great Eastern Japan Earthquake, it was a common phenomenon that bridge piers collapsed at the bottom of pier columns, so in this chapter, a comparison of acting moment and resistant moment at the bottom of the piers was presented to demonstrate the damage condition of piers. Considering that the wave effect on the middle span of the bridge was strongest, P8 is shown as an example.

In order to calculate the acting moment at the bottom (section A) of column, all of the external forces on P8 were found. As being illustrated in **Fig.18**, the external forces affected on Pier 8 have been divided into 2 types. The first type (F1) is wave-induced acting force, which affected on the side area of pier, and is able to be determined by Equation (8)[5]. Before retrofit, the wave pressure area of P8 is 1.8m×7.1m.

$$P = K \cdot v^2 \cdot A \quad (8)$$

Where,

P is wave acting force (kN); K is the coefficient determined by the shape of piers (assumed as 0.7 according to the Japanese Specification[4]); v is wave flow velocity (6.0m/s); A is wave pressure area on piers

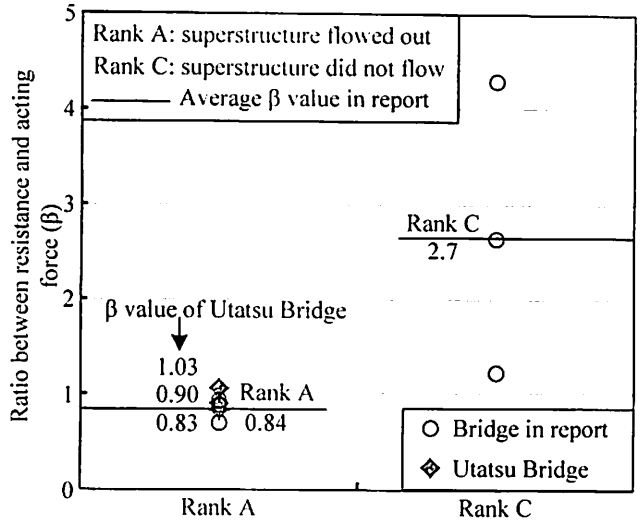

Fig.17 Comparing β Values with Report

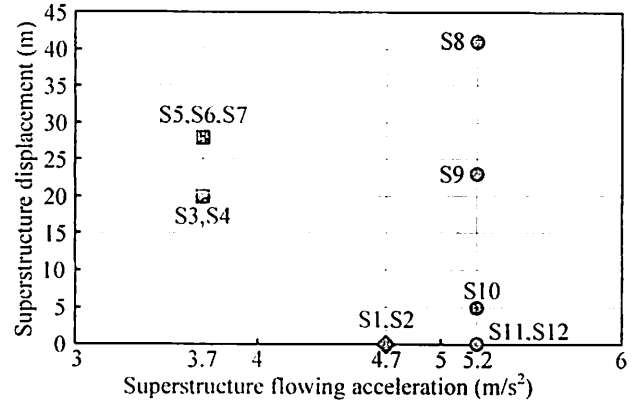

Fig.18 Relation between Superstructure Flowing acceleration and Displacement

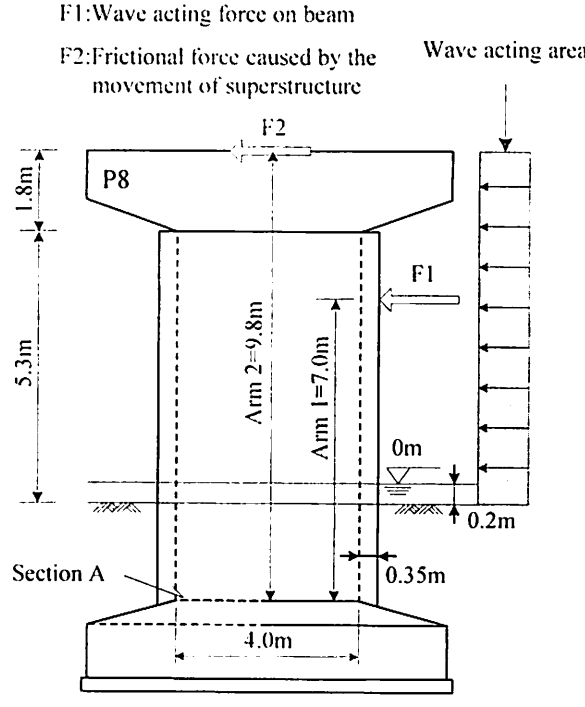

Fig.19 Acting Forces on P8

The second type of acting force is the frictional force imposed by the movement of the superstructure upon P8. This type could be determined by using the Equation (3) which has been accomplished in Chapter 2. After these 2 external forces determined, the moment arms of them were searched according to the Japanese specification[4]. In the end, both 2 acting moments caused by F1 and F2 could be determined and the result is shown in **Table.1**. The total acting moment on section A was calculated as 22250 kN·m. The column of P8 has been retrofitted with the reinforcement concrete surface, as shown in **Fig.18 (b)**, so the wave pressure area became 2.5m×7.1m. And by the same method, the total acting moment was calculated as 23132 kN·m.

Aiming at checking the P8's strength at an extreme adverse situation, the authors assume the superstructure collapse preventions hold sufficient resistance to prevent the flow of superstructures on P8. In this case, F2 would become the wave acting force on the superstructures on P8. By the same method above, the total acting moment was calculated as 29208 kN·m (before retrofit) and 30090 kN·m (after retrofit), shown in **Fig.19**.

Based on the dimensions of section A (before retrofit), 4.0m (width) ×1.8m (height), and the reinforcement at section A: SD295D13ctc150, assumed based on the similar piers, the resistant moment has been obtained as 24000 kN·m. Nevertheless, if take the retrofit of the reinforcement concrete surface into account, the resistant moment becomes 60000 kN·m, refer to **Fig.19**. Obviously, the resistant moment after retrofit is sufficient to prevent P8 collapsing even for the extreme situation assumed. By the same method, the damage condition of all piers could be evaluated. Then after retrofit, all piers kept enough strength to resist collapse.

6. CONCLUCUSIONS

From the field survey and the comparison between the wave acting force and the resistance, the conclusions have been stated below:

(1) Based on the field survey, for the damage of superstructures, S3~S10 experienced serious dislocations. For the damage of piers, all piers did not collapse and the main damage is that their superstructure collapse preventions flowed out.

(2) The values of ratio β between superstructure resistance and wave acting force respectively are 0.90, 1.03 and 0.83. Comparing with the average β value (0.84) of the bridges, located at the Tohoku region, which suffered serious dislocations, the β values of the Utatsu Bridge are close to rank A. So it is easy for S3~S10 to flow out under the wave force in horizontal direction.

(3) By the comparison of the wave acting moment and the resistant moment, after retrofit, at the bottom (section A) of Pier 8, as an example, it was summarized that the resistant moment is 2.0 times stronger than the acting moment of the extreme situation assumed, so P8 did not collapse. By the same method, it can be verified that all piers kept sufficient strength to prevent collapse.

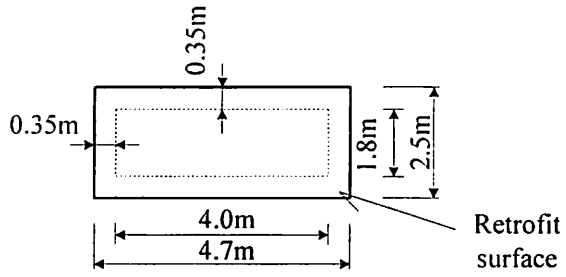

Fig.20 Cross Section of Column

Table.1 Calculation of Acting Moment

The data in () are after retrofit

Acting Force Number	Acting Force (kN)	Moment Arm (m)	Acting Moment (kN·m)
F1	322.6 (448.6)	7.0	2258 (3140)
F2	2040	9.8	19992
Total			22250 (23132)

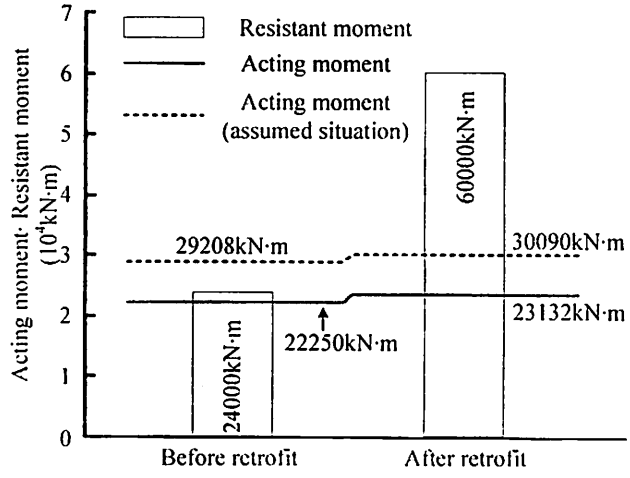

Fig.21 Comparison of Acting Moment and Resistant Moment

REFERENCES

1) Kosa, K., Nii, S., Shoji G., Miyahara K.,: Analysis of Damaged Bridge by Tsunami due to Sumatra Earthquake, Journal of Structural Engineering, Vol.55A, pp .456-460, 2010.3

2) Japan Road Association, "Specifications for Highway Bridges Part I Common", pp .52, 2002.3

3) Shoji, G., Moriyama, T., Fujima K., Shigihara Yo., Kasahara, K.,: Experimental Study Associated with A Breaking Tsunami Wave Load Acting onto A Single Span Bridge Deck, Journal of Structural Engineering, Vol.55A, pp .460-470, 2009.4

4) The Earthquake Engineering Committee, JSCE.,: The Urgent Damage Survey Report of Great Eastern Japan Earthquake, Chapter 9, pp. 90-91, 2011.5

5) Japan Road Association, "Specifications for Highway Bridges Part I Common", pp .43-44, 2002.3